Applied Energy 113 (2014) 751–757

Contents lists available at ScienceDirect

Applied Energy

journal homepage: www.elsevier.com/locate/apenergy

Effect of a homogeneous combustion catalyst on the characteristics of diesel soot emitted from a compression ignition engine

Yu Ma, Mingming Zhu, Dongke Zhang *

Centre for Energy (M473), The University of Western Australia, 35 Stirling Highway, Crawley, WA 6009, Australia

HIGHLIGHTS

- The effect of a ferrous picrate catalyst on soot characteristics was investigated.
- Primary soot and aggregates from the catalyst treated diesel were smaller in size.
- The soot from the catalyst treated diesel possessed higher C/H and C/O ratios.
- The catalyst promotes fuel combustion, leading to less soot precursors.
- The catalyst actively accelerates the soot oxidation process.

ARTICLE INFO

Article history:
Received 7 June 2013
Received in revised form 8 August 2013
Accepted 10 August 2013
Available online 3 September 2013

Keywords:
Compression ignition engines
Diesel soot
Homogeneous combustion catalyst
Iron
Soot oxidation

ABSTRACT

The effect of a ferrous picrate based homogeneous combustion catalyst (FPC), known to improve diesel combustion efficiency, on the morphological and chemical characteristics of diesel soot was studied in detail. Diesel soot samples emitted from a laboratory CI engine fuelled with a commercial diesel, with and without FPC doping, were collected and characterised using a combination of several advanced analytical techniques including a TEM fitted with EELS, an FT-IR, and a solid state ^{13}C NMR, in addition to elemental analysis. Compared to the soot from the reference diesel, the soot particle sizes of both primary soot and aggregates from the FPC treated diesel were consistently smaller and decreased with increasing FPC dosage. Both types of soot showed similar fractal dimensions, indicating that there were no apparent changes in the formation mechanisms of the primary soot particles and their agglomeration processes. Furthermore, the types of the carbon bonds and organic functional groups in the soot were virtually unaffected by FPC, as indicated by the similar degrees of graphitisation and indistinguishable chemical structures in the two types of soot. However, the soot from the FPC treated diesel showed slightly higher C/H and C/O ratios than those from the reference diesel. Based on these observations, it was speculated that FPC enhanced the diesel combustion process, leaving fewer soot precursors, and also promoted the oxidation of soot particles, resulting in smaller sizes of the primary soot and aggregates and reduced the overall soot emissions.

1. Introduction

The emissions of particulate matter, normally known as soot, from compression ignition (CI) engines are under increasing scrutiny because of its eminent risks to human health and the environment [1–3]. Literature reports have shown that the particle size, morphology and chemical composition of soot are directly related to their formation, transport, optical and deposition properties [4,5]. Generally speaking, diesel soot is chain-like clusters or aggregates of spherical-shaped primary particles, varying widely in size. The complex morphologies of soot can be described by fractal dimension [6]. In terms of chemical composition, soot is a solid carbonaceous substance formed in fuel-rich regions during the combustion of hydrocarbons, with unburned hydrocarbons, trace metals and sulphates absorbed on their surfaces [7].

It is widely accepted that during combustion, the formation of soot particles can be depicted in six sequential steps [6–9]: (1) upon intense heating, the pyrolysis of hydrocarbons takes place to generate unsaturated hydrocarbons, acetylenes and polycyclic aromatic hydrocarbons (PAH) as soot formation precursors; (2) the soot precursors nucleate to form larger PAH molecules; (3) the reactive surface of the nucleated soot particles continues to grow by attracting and interacting with gas-phase molecular fragments of hydrocarbons; (4) coagulation and coalescences of the large molecular fragments take place by collision to form spherical primary soot particles; (5) agglomeration of the primary particles occurs to form large aggregates with chain-like structures; and

* Corresponding author. Tel.: +61 8 6488 7600; fax: +61 8 6488 7235.
E-mail address: dongke.zhang@uwa.edu.au (D. Zhang).

0306-2619/$ - see front matter © 2013 Elsevier Ltd. All rights reserved.
http://dx.doi.org/10.1016/j.apenergy.2013.08.028

finally (6) the oxidation of the soot particles happens concurrently with the soot formation. In diffusion flames (such as those in CI engines), oxidation of soot occurs subsequently to the soot formation process. In CI engine systems, soot normally forms in fuel-rich regions with air deficiencies, and can also be viewed as an indication of poor combustion efficiency [10,11]. The actual soot formation process is complex and associated with many factors, such as fuel structure and composition, engine design, as well as the engine operation and environmental conditions.

To meet the increasingly stringent regulations, numerous efforts have been made to control the diesel soot emissions by modifying the engine systems, developing post-combustion treatment devices, and improving fuel formulations [2,12,13], or by combinations of these approaches. One effective alternative is to add a catalyst to the diesel fuel. The catalyst usually contains a metallic part to promote the fuel combustion and an organic part to make the catalyst soluble in diesel, thus the term homogeneous combustion catalysts (HCCs). Laboratory and modelling studies [14–17] have shown that the addition of trace amounts of such catalysts can significantly improve combustion efficiency and reduce pollutant emissions from CI engines. Some authors [18–20] have also claimed that these catalysts can be used in conjunction with diesel particulate filter (DPF) to help lower the soot oxidation temperature and thus facilitate the DPF regeneration process. In practical applications, HCCs generally feature the following characteristics: (1) they are commercially available, cost-effective, less-corrosive and chemically stable during storage and on-board usage; (2) they can be homogeneously dissolved in diesel fuel without phase separation, acting as catalytic agents to promote the combustion process with substantial fuel savings and emission reduction; (3) they are added to diesel at ultra-low ratios (ppm levels) with no discernible changes in fuel properties and minimal effects on fuel delivery line and injection system and other engine parts and (4) the use of HCCs does not introduce new harmful substances nor incur secondary pollutions to life and the environment [21].

Our previous work [22,23] has focused on an iron-based HCCs, called FPC with ferrous picrate as the active ingredient, capable of reducing up to 39% soot, 21% CO, 13% unburned hydrocarbon emissions and saving up to 4.2% brake specific fuel consumptions from a CI engine under the conditions tested. As the level of smoke emission was determined using an opacimeter [22,23], the measured reduction in the soot is lineally correlated with the particle number density in the exhausts. Therefore, the decreased smoke emission indicates that the total number of soot particles is also significantly reduced due to the use of FPC. Further analyses using a thermogravimetric analyser (TGA) and transmission electron microscopy (TEM) [24] showed higher oxidative reactivity and smaller primary particle size possessed by the soot from the FPC treated diesel. However, there is a lack of knowledge if the FPC addition would alter the detailed physical and chemical properties of the soot particles.

Understanding the characteristics of diesel soot is crucial for evaluating its impacts on human health and the environment [5] and, on the other hand, can also provide insights into the mechanisms of the catalyst in diesel combustion and soot formation processes. There are a number of analytical techniques available for soot characterisations. Transmission electron microscope (TEM) has been extensively used to ascertain the nanostructure and fractal properties of soot particles, as well as to determine the sizes and distributions of the primary soot and aggregates [25,26]. Chemical structure and elemental composition of soot have often been analysed using one or a combination of electron energy loss spectroscopy (EELS), Fourier transform infra-red spectroscopy (FT-IR), solid state nuclear magnetic resonance (NMR) spectroscopy and elemental analysers [27–29]. In the present work, a combination of all of the above analytical techniques was employed to provide more detailed and comprehensive information about the nature of the soot collected from the exhausts of a laboratory CI engine fuelled with a reference diesel and the FPC treated diesel. The detailed morphological, structural and compositional features thus revealed would allow a much improved understanding of the characteristics of soot, providing a thorough assessment of the influence of FPC in diesel soot formation process.

2. Experimental

2.1. Materials

A commercial diesel from a local service station (Caltex Australia) was used as the reference diesel. A ferrous picrate catalyst (FPC) was a homogeneous solution of ferrous picrate dissolved in a solvent mix including high alcohols, short-chain alkyl benzene and other aromatics [18–20]. The catalyst was added to the reference diesel at two dosing ratios, 1:10,000 and 1:1000 by volume. The three fuel samples were then tested in a laboratory CI engine, from which respective soot particles were collected and subjected to subsequent analysis and characterisation. For convenience, the reference diesel was denoted as "RD", while the two catalyst-treated fuels were abbreviated as "FPC-D (1:10,000)" and "FPC-D (1:1000)", respectively.

2.2. Test engine and soot collection

The engine and soot collection system have been reported elsewhere [24]. Briefly, a four-stroke, single cylinder, direct injection CI engine (YANMAR L48AE, AET Ltd.) was employed to generate the soot particles. The engine had a 70 mm bore, 55 mm stroke, 211 cm^3 displacement and compression ratio of 19.9:1. A Zöllner Type A-100, water cooled, electric dynamometer was coupled to the engine output shaft to provide the load conditions. During soot collection, the engine was maintained under steady-state with 2800 rpm speed and 5.5 Nm load (equivalent to 75% of the maximum load). Note that key objective of this work was to investigate the effect and mechanisms of FPC in soot formation and oxidation processes in CI engines and it was considered desirable to run the engine at a single operation point of 75% of maximum load to enable consistent sampling of the soot for detailed characterisation also consistent with our previous publication [24]. This is justified as the engine operating conditions would not significantly alter the catalytic mechanisms. When the engine was stabilised, a glass fibre filter paper (Whatman GF/A, 1.6 μm pore size) supported on a ceramic holder was inserted perpendicular to the exhaust path to collect bulk soot for three hours. The soot was scratched off the filter paper and stored in a desiccator for further analysis. For TEM imaging, the soot particles were directly sampled from the exhaust using a thermophoretic sampling technique as described elsewhere [24]. In brief, a 30 mm-long grid holder with TEM copper grids (200 mesh, holey carbon film coating) attached to the tip was inserted parallel to the exhaust stream by a step motor for rapid sample collection. Three samples were taken consecutively for each fuel run to ensure the repeatability of the subsequent sample analysis.

2.3. Analysis and characterisation

The morphological feature and size of soot particles were determined using a JEOL 2100 TEM operating at accelerating voltage of 120 kV and magnifications from 5000× to 50,000×. The images acquired were processed using DigitalMicrograph software (Gatan Inc.). These 2-D images were found to be sufficient to reveal 3-D

features, including sizes and size distribution of the primary soot and aggregates, and the fractal dimensions of the soot particles.

The types of the carbon–carbon bonds in the soot were ascertained by operating the JEOL 2100TEM in EELS mode. Prior to the analysis, the sample grids were preheated in vacuum at 50 °C to eliminate volatile contaminants absorbed on the soot particles [30]. For each sample, the EELS measurements were performed on a circular region (0.13 μm^2) of the soot without the underlying carbon film, and ten spectra were randomly acquired from different regions of the sample. The EEL spectra were recorded using a Gatan Tridiem energy filter with an energy resolution of 1.7 eV (full width at half maximum of the zero loss peak) and a dispersion rate of 0.1 eV per pixel. Subsequently, the spectra were background-subtracted using the DigitalMicrograph software and an averaged value was presented for each soot sample.

Organic functional groups in the soot were analysed using a Nicolet 6700 FT-IR spectrometer (Thermo Scientific) in a wavelength range of 500–3600 cm^{-1} with a resolution of 0.09 cm^{-1}. A thin and homogenous KBr pellet was prepared with 0.2 wt.% of each soot sample. An accumulation of 100 scans was set to obtain the spectra with optimum resolution.

Solid state ^{13}C cross polarisation magic angle spinning (CP/MAS) NMR spectra of the soot were obtained using a Varian 400 NMR spectrometer at a frequency of 100.6 MHz. Around 100 mg of each soot sample was packed individually in a cylindrical zirconia rotor with 4 mm diameter and spun at the magic angle (54.7 °C) at 5000 ± 5 Hz. The chemical shifts were externally referenced to adamantane (29.5 ppm). All spectra acquired were zero fitted to 8192 data points and processed by the Lorentzian line broadening method.

All soot samples were also analysed for their elemental compositions. Up to 30 mg of each sample was packed into a container and examined using a Perkin–Elmer Model 2400 CHN/O elemental analyser for simultaneous measurements of carbon, hydrogen, nitrogen and ash. To determine the sulphur contents, soot samples were digested in a HNO_3-HF mixture and analysed by an iCAP 6500 inductively coupled plasma–atomic emission spectrometry (ICP-AES, Thermo Scientific). Each sample was analysed twice and reproducibility was assured. The oxygen content was determined by balance [31].

3. Results and discussion

3.1. Soot morphology, particle size and fractal dimension

Fig. 1 displays typical TEM micrographs of diesel soot. Fig. 1(a) shows an image of a soot aggregate at high-magnification. It can be seen that the soot aggregate exhibited a grape- [32] or chain-like [33] structure, and consisted of hundreds of spherical, primary soot with fairly uniform diameters. In contrast, as the low-magnification image shown in Fig. 1(b), the soot aggregates had clearly non-uniform sizes and irregular shapes. According to Heywood [34], the non-homogeneous nature of CI engine combustion leads to the formation of soot particles of different ages, which escape from the cylinder. Thus the soot aggregates of various sizes and shapes co-exist in the exhausts. In general, there were no remarkable differences in terms of the morphologies as revealed by the TEM images, between the soot collected from RD and FPC treated fuels.

The size distributions of primary soot particles from the three fuel runs were determined using the method reported elsewhere [24], which measures the particle diameter (D_p) by imposing circular outlines over the spherical primary soot isolated on the TEM image. The uncertainty of this measurement method is associated with the deviation of the TEM instrument in obtaining the micro-

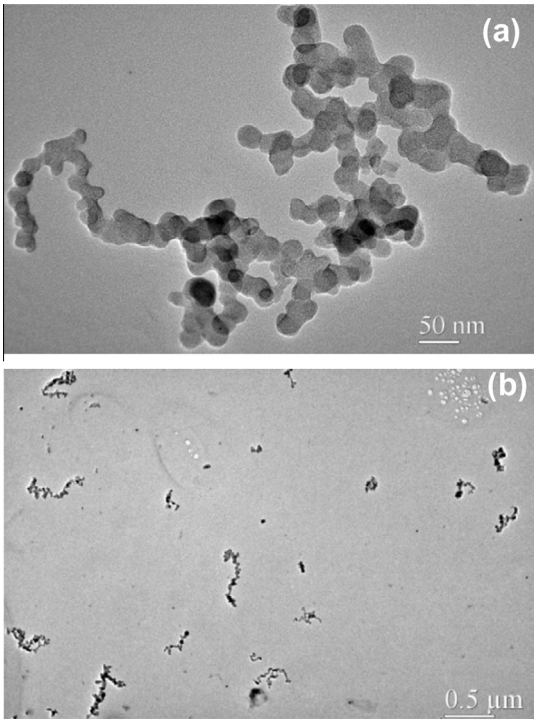

Fig. 1. TEM images at the magnifications of (a) 50,000× and (b) 5000× of typical diesel soot particles sampled from the exhausts of the engine fuelled with RD at 2800 rpm speed and 5.5 Nm load.

scopic images of soot particles, which is at ±2% of the true value [35,36]. In Fig. 2, it can be seen that all primary soot particles displayed typical Gaussian distributions, and their sizes generally ranged from 10 to 55 nm, in agreement with the literature reports [26,29,35]. The average diameter $\overline{D_p}$ for the RD soot was found to be 24.5 nm, but was 23.5 nm and 20.7 nm for the soot from FPC-D (1:10,000) and FPC-D (1:1000), respectively, consistently demonstrating that the FPC has influenced the primary particle size during the combustion process [20].

After knowing $\overline{D_p}$ of the soot, the fractal dimension D_f was determined to reveal the agglomeration and growth mechanisms of the soot particles. It is well established that D_f can be obtained from the following power–law equation [25,26,36],

$$N = k_f \left(\frac{D_g}{\overline{D_p}}\right)^{D_f} = k_L \left(\frac{L}{\overline{D_p}}\right)^{D_f} \quad (1)$$

where N is the number of primary soot in an aggregate; D_g and L the gyration diameter and length of an aggregate; k_L a constant correlating with the fractal pre-factor k_f by,

$$\frac{k_f}{k_L} = \left(\frac{L}{D_g}\right)^{D_f} = \left(\frac{D_f + 2}{D_f}\right)^{D_f/2} \quad (2)$$

N can be estimated from the following empirical equation [26,36,37],

$$N = 1.15 \left(\frac{A_a}{\overline{A_p}}\right)^{1.09} \quad (3)$$

where A_a is the cross-sectional area of the aggregate; $\overline{A_p}$ is the cross-sectional area of the primary soot particle, determined by $\overline{A_p} = \pi \overline{D_p}^2/4$.

After measuring A_a and L of about 100 soot aggregates from TEM images, the fractal dimension D_f was acquired by calculating the slop of the least-square fit to the double-logarithmic plot of

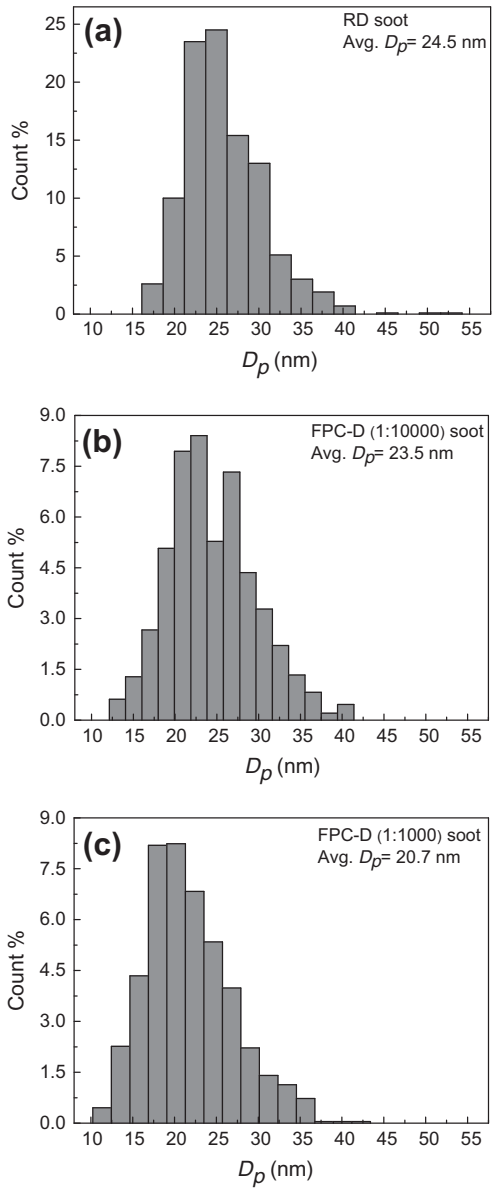

Fig. 2. Primary particle size distributions of soot sampled from the exhausts of the engine fuelled with (a) RD, (b) FPC-D (1:10,000), and (c) FPC-D (1:1000).

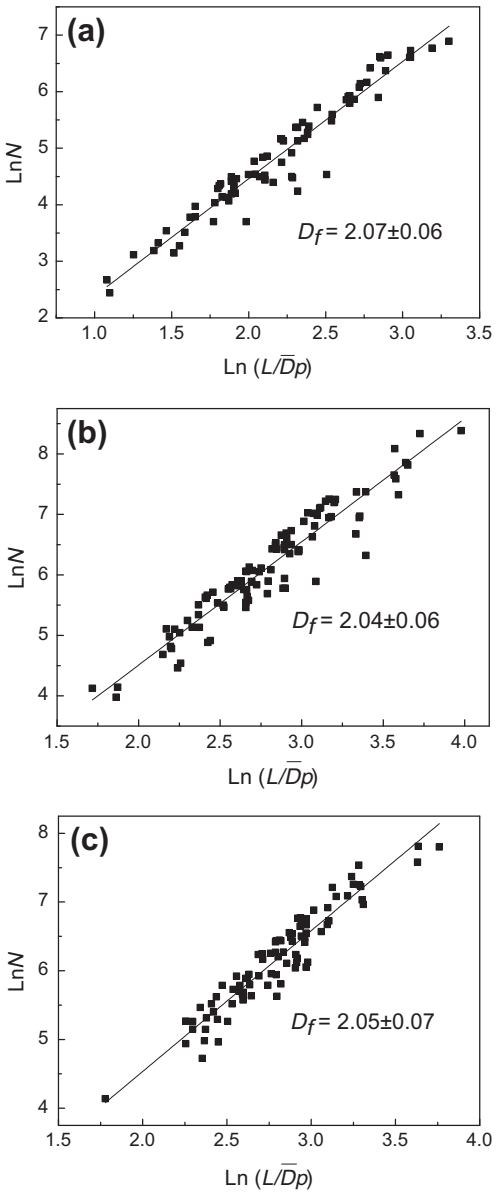

Fig. 3. Fractal dimensions of soot sampled from the exhausts of the engine fuelled with (a) RD, (b) FPC-D (1:10,000), and (c) FPC-D (1:1000).

N versus $L/\overline{D_p}$, as shown in Fig. 3. The double-logarithmic distributions of N and $L/\overline{D_p}$ yielded a perfect linear fit. Moreover, D_f of the three soot samples were found to be at similar values of around 2. According to Meakin [38], D_f above 1.8 implies that the soot particles are formed under a cluster–cluster growth mode. In CI engines, the primary soot grows by monomer–cluster collisions at the early stage of soot formation, due to the presence of a large quantity of monomers from hydrocarbon pyrolysis [39]. As the particle agglomeration occurs and consumes most of the monomers, the cluster–cluster growth mode dominates the formation of the soot aggregates [39]. The similar values of the fractal dimensions of soot from diesel with and without FPC indicates that the way the soot aggregates were formed was unaffected by the catalyst addition.

Soot aggregates in various shapes and sizes were characterised by gyration diameter D_g, according to Eq. (2). As shown in Fig. 4, D_g of the soot samples scattered among 85–645 nm, confirming that the soot aggregates were distributed over a wide range. In comparison to that of the RD soot, the average D_g was found to be smaller for the soot from the FPC treated fuels, and further decreased with increasing the catalyst dosage. Statistically, 90% of the aggregates were below 477 nm in sizes for the RD soot, but were below 436 nm and 378 nm for soot from FPC-D (1:10,000) and FPC-D (1:1000), respectively.

3.2. Chemical structure in soot

Fig. 5 presents the EEL spectra of soot from diesel with and without FPC treatment. The spectra generally show two distinct peaks. The sharp peak at the lower energy of 285 eV is attributed to the sp^2 (π^*) hybridised carbon bond, as often referred to "graphite peak" [27]. The broad peak at the higher energy of 292 eV corresponds to the sp^3 (σ^*) hybridised carbon bond [29]. The peak intensity ratio I_{π^*}/I_{σ^*} is proportional to the degree of graphitisation of the soot, where a higher value indicates a pronounced π bonding with a greater structural graphitic character. In Fig. 5, it is noted that all soot samples possessed similar I_{π^*}/I_{σ^*} values, being 0.584 ± 0.007 for the RD soot in comparison to 0.582 ± 0.006 and 0.580 ± 0.007 for soot from FPC-D (1:10,000) and FPC-D (1:1000),

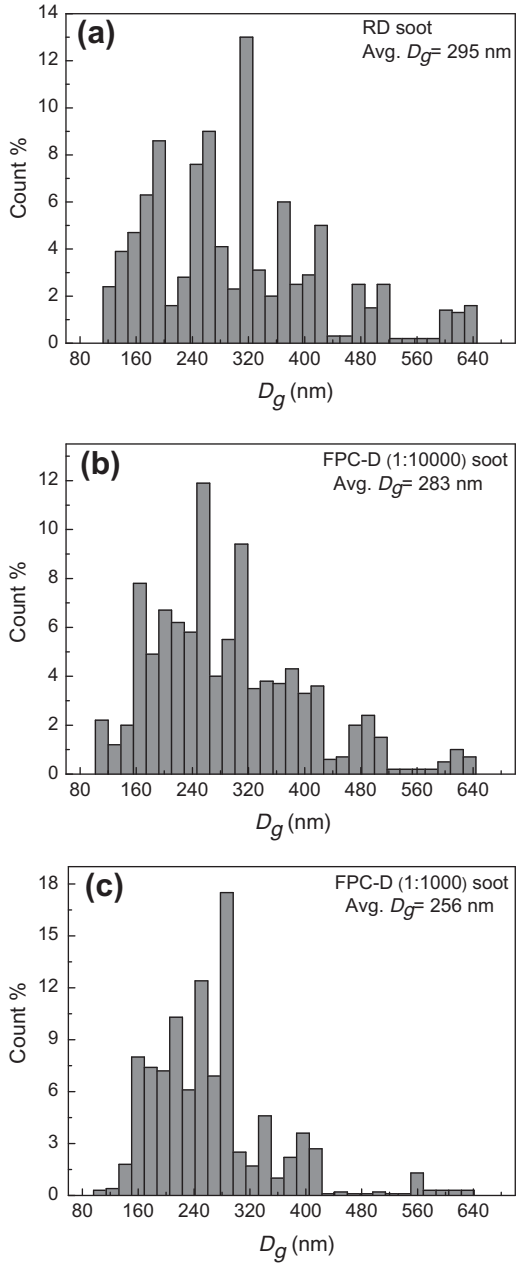

Fig. 4. Aggregate size distributions of soot sampled from the exhausts of the engine fuelled with (a) RD, (b) FPC-D (1:10,000), and (c) FPC-D (1:1000).

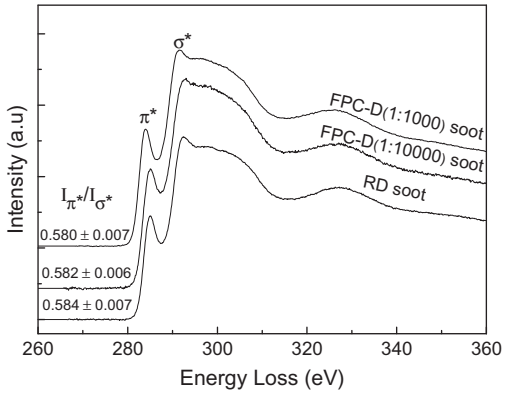

Fig. 5. EEL spectra of soot sampled from the exhausts of the engine fuelled with RD, FPC-D (1:10,000) and FPC-D (1:1000).

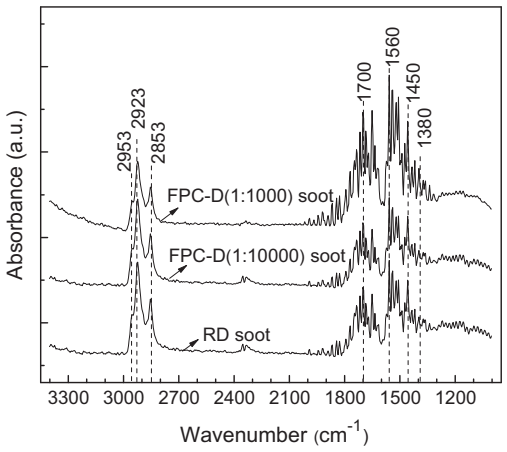

Fig. 6. FT-IR spectra of soot sampled from the exhausts of the engine fuelled with RD, FPC-D (1:10,000) and FPC-D (1:1000).

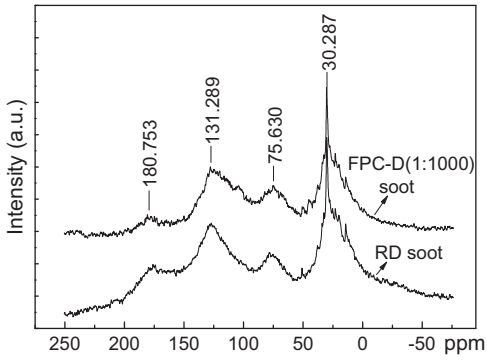

Fig. 7. Solid state ^{13}C CP/MAS NMR spectra of soot sampled from the exhausts of the engine fuelled with RD and FPC-D (1:10,000).

Table 1
Distribution of organic functional groups in soot samples as estimated from the CP/MAS ^{13}C NMR spectra.

Sample	*Chemical shift range (ppm)*			
	Alkyl C 0–50	O-Alkyl C 50–110	Aryl C 110–160	Carbonyl C 160–200
RD soot	37	20	30	13
FPC-D (1:1000) soot	38	17	30	15

Table 2
Elemental compositions (by weight percentage) of soot samples from RD and FPC-D (1:1000).

	RD soot	FPC-D (1:1000) soot
C	82.52	83.52
H	6.46	5.90
N	0.50	0.52
S	0.13	0.18
O[a]	10.31	9.80
Ash	0.08	0.08
$(C/H)_{total}$[b]	1.06	1.18
$(C/O)_{total}$[b]	10.67	11.36

[a] O content was determined by difference.
[b] Referring to the total molar ratios of C/H and C/O in the soot.

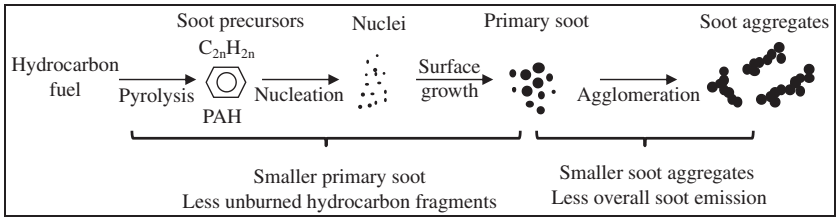

Fig. 8. A schematic of the proposed mechanism of the FPC catalyst in soot formation processes.

respectively. This suggests that FPC caused no discernible differences in the degree of graphitisation. This observation confirms that the soot building units were unaffected by the catalyst addition, consistent with previous HRTEM analyses [24].

Fig. 6 shows the FT-IR spectra of the RD soot and soot from the FPC treated fuels. Major characteristic peaks are marked out, representing the C—H asymmetric and symmetric stretching of aliphatic groups at 2953 cm^{-1}, 2923 cm^{-1} and 2853 cm^{-1}, C—O stretching of carbonyl groups at 1700 cm^{-1}, C=C stretching of aromatics and alkenes at 1560 cm^{-1}, and aliphatic C—H plane deformation of CH_2/CH_3 groups at 1450 cm^{-1} and 1380 cm^{-1} [28,40]. It is noted that the three soot samples featured similar peak patterns over the wavelength range, indicating that the types of organic functional groups in the soot were not significantly altered by FPC.

Fig. 7 compares the CP/MAS NMR spectra of the RD soot and the FPC-D (1:1000) soot. The strongest peak with the chemical shift centred at around 30 ppm was attributed to the alkyl C, while the peak centred at 131 ppm was assigned to the aromatic C, with the small bands at 75 ppm and 180 ppm corresponding to the alkyl C—O and carbonyl C=O groups, respectively [27,41]. It was obvious that the spectra of the two samples showed a similar trend, suggesting that there were no remarkable differences in terms of chemical structures in the soot from diesel with and without FPC treatment.

The distribution of the functional groups identified in the CP/MAS NMR spectra was estimated by integrating the signal intensities over the characteristic regions, with the results shown in Table 1. It can be seen that the FPC-D (1:1000) soot possessed similar amounts of the functional groups to those in the RD soot. Note that the NMR results in the present study were of semi-quantitative nature. According to the literature [42,43], the intrinsic uncertainty of the analysis was associated with the quantification of the aryl C groups, due to the relatively high field NMR spectrometer (400 MHz) used. Therefore, elemental analysis with high quantitative accuracy was introduced to characterise the soot samples.

3.3. Elemental composition of soot

The elemental analysis results of soot from RD and FPC-D (1:1000) are shown in Table 2. There were no significant differences in the *N*, *S* and ash contents between the two types of soot. However, it may be noted that the proportions of the elemental H and O were slightly decreased and the elemental C increased for the FPC-D (1:1000) soot, resulting in higher C/H and C/O ratios compared to those of the RD soot. Typically, the H and O contents in soot can be viewed as signs of unburned hydrocarbons and oxygenated compounds (e.g. carbonyls, ethers), which are generated as by-products due to incomplete combustion [28,31]. The higher C/H and C/O ratios of the FPC-D (1:1000) soot implied that the FPC catalyst promoted diesel combustion, resulting in an improved combustion efficiency and therefore fewer unburned hydrocarbons and oxygenated compounds were formed and attached to the soot particles.

3.4. The effect of FPC in soot formation

Summarising the aforementioned discussion and interpretation of the present results, along with those reported in the literature, a plausible mechanism of the FPC catalyst in diesel combustion and soot formation processes in CI engines was proposed, as illustrated in Fig. 8. During diesel combustion, the catalyst can effectively improve the combustion efficiency, resulting in a higher peak cylinder pressure, faster heat release rate and significantly reduced fuel consumption [22]. In this improved combustion environment, the hydrocarbon fragments from fuel pyrolysis burn more completely, leaving fewer soot precursors and thus leading to smaller primary soot and aggregates. In these steps, the formation mechanisms of the primary soot and aggregates remain unaffected by the catalyst, as indicated by the similar fractal dimensions and functional groups in the soot from diesel with and without the FPC treatment. In the later stage of combustion, the catalyst effectively promotes the soot oxidation, which is inferred by the lower ignition temperature and higher oxidation rates of the soot from the FPC treated fuels [24]. Following the aforementioned mechanism, diesel combustion in CI engines is substantially improved by the catalyst, resulting in soot particles with higher C/H and C/O ratios and less overall soot emissions.

4. Conclusions

The effect of a ferrous picrate based homogeneous combustion catalyst on the morphological, structural and compositional properties of soot from a CI engine has been extensively examined using a combination of several advanced analytical techniques. The sizes of both primary soot and aggregates from the FPC treated diesel were found to be smaller and further decreased by increasing the FPC dosage. The nanostructure and fractal dimension remained the same for the soot from the FPC treated fuels compared to those of the RD soot, indicating that the formation mechanisms of the primary soot and aggregates remained unaffected by the catalyst. Similarities in the degree of graphitisation and chemical structures were also found between the soot from diesel with and without FPC treatment, suggesting that the types of carbon bonds and organic functional groups in soot were not significantly altered. However, higher C/H and C/O ratios were identified for the soot from the FPC treated diesel, indicating that less unburned hydrocarbons and oxygenated compounds were formed and absorbed onto the soot.

The mechanism of the FPC in CI engine combustion was proposed in that, the catalyst promotes fuel combustion, leaving less hydrocarbon fragments to form soot precursors, thus the smaller primary soot and aggregates. In the later stage of combustion, the catalyst actively accelerates the soot oxidation process. As a result of improved combustion, the soot showed higher C/H and C/O ratios and was reduced in the overall emission. This postulation provides a plausible interpretation of the mechanism of the cata-

lyst in improving the fuel efficiency and reducing the overall soot emissions from CI engines.

Acknowledgements

This research was supported by the Australia Research Council under the ARC Linkage Projects Scheme (Project Number: LP0989368) in partnership with Fuel Technology Pty Ltd. and BHP Billiton Iron Ore Pty Ltd.

References

[1] Kittelson DB. Engines and nanoparticles: a review. J Aerosol Sci 1998;29:575–88.
[2] Lloyd AC, Cackette TA. Diesel engines: environmental impact and control. J Air Waste Manage 2001;51:809–47.
[3] Burtscher H. Physical characterization of particulate emissions from diesel engines: a review. J Aerosol Sci 2005;36:896–932.
[4] Broday DM, Rosenzweig R. Deposition of fractal-like soot aggregates in the human respiratory tract. J Aerosol Sci 2011;42:372–86.
[5] Berube KA, Jones TP, Williamson BJ, Winters C, Morgan AJ, Richards RJ. Physicochemical characterisation of diesel exhaust particles: factors for assessing biological activity. Atmos Environ 1999;33:1599–614.
[6] Smith OI. Fundamentals of soot formation in flames with application to diesel engine particulate emissions. Prog Energy Combust Sci 1981;7:275–91.
[7] Tree DR, Svensson KI. Soot processes in compression ignition engines. Prog Energy Combust Sci 2007;33:272–309.
[8] Glassman I. Soot formation in combustion processes. In: Symposium (international) on combustion, vol. 22; 1988. p. 295–311.
[9] Mosbach S, Celnik MS, Raj A, Kraft M, Zhang HR, Kubo S, et al. Towards a detailed soot model for internal combustion engines. Combust Flame 2009;156:1156–65.
[10] Hall-Roberts VJ, Hayhurst AN, Knight DE, Taylor SG. The origin of soot in flames: is the nucleus an ion? Combust Flame 2000;120:578–84.
[11] Wang H. Formation of nascent soot and other condensed-phase materials in flames. Proc Combust Inst 2011;33:41–67.
[12] Knecht W. Diesel engine development in view of reduced emission standards. Energy 2008;33:264–71.
[13] Johnson TV. Diesel emission control in review. SAE technical paper no 2006–01-0030; 2006.
[14] Yang HH, Lee WJ, Mi HH, Wong CH, Chen CB. PAH emissions influenced by Mn-based additive and turbocharging from a heavy-duty diesel engine. Environ Int 1998;24:389–403.
[15] Chlopek Z, Darkowski A, Piaseczny L. The influence of metalloorganic fuel additives on CI engine emission. Polish J Environ Stud 2005;14:559–67.
[16] Skillas G, Qian Z, Baltensperger U, Matter U, Burtscher H. The influence of additives on the size distribution and composition of particles produced by diesel engines. Combust Sci Technol 2000;154:259–73.
[17] Keskin A, Guru M, Altiparmak D. Influence of metallic based fuel additives on performance and exhaust emissions of diesel engine. Energy Convers Manage 2011;52:60–5.
[18] Valentine JM, Peter-Hoblyn JD, Acres GK. Emissions reduction and improved fuel economy performance from a bimetallic platinum/cerium diesel fuel additive at ultra-low dose rates. SAE technical paper no 2000–01-1934; 2000.
[19] Song JH, Wang JG, Boehman AL. The role of fuel-borne catalyst in diesel particulate oxidation behavior. Combust Flame 2006;146:73–84.
[20] Okuda T, Schauer JJ, Olson MR, Shafer MM, Rutter AP, Walz KA, et al. Effects of a platinum–cerium bimetallic fuel additive on the chemical composition of diesel engine exhaust particles. Energy Fuel 2009;23:4974–80.
[21] Haycock R, Thatcher R. Fuel additives and the environment. Document 52 revision, the technical committee of petroleum additive manufacturers in Europe (ATC); 2004.
[22] Zhu M, Ma Y, Zhang D. Effect of a homogeneous combustion catalyst on the combustion characteristics and fuel efficiency in a diesel engine. Appl Energy 2012;91:166–72.
[23] Ma Y, Zhu M, Zhang D. The effect of a homogeneous combustion catalyst on exhaust emissions from a single cylinder diesel engine. Appl Energy 2013;102:556–62.
[24] Zhang D, Ma Y, Zhu M. Nanostructure and oxidative properties of soot from a compression ignition engine: the effect of a homogeneous combustion catalyst. Proc Combust Inst 2013;34:1869–76.
[25] Koylu UO, Faeth GM, Farias TL, Carvalho MG. Fractal and projected structure properties of soot aggregates. Combust Flame 1995;100:621–33.
[26] Neer A, Koylu UO. Effect of operating conditions on the size, morphology, and concentration of submicrometer particulates emitted from a diesel engine. Combust Flame 2006;146:142–54.
[27] Jager C, Henning T, Schlogl R, Spillecke O. Spectral properties of carbon black. J Non-Cryst Solids 1999;258:161–79.
[28] Salamanca M, Mondragon F, Agudelo JR, Benjumea P, Santamaria A. Variations in the chemical composition and morphology of soot induced by the unsaturation degree of biodiesel and a biodiesel blend. Combust Flame 2012;159:1100–8.
[29] Al-Qurashi K, Boehman AL. Impact of exhaust gas recirculation (EGR) on the oxidative reactivity of diesel engine soot. Combust Flame 2008;155:675–95.
[30] Ritrievi KE, Longwell JP, Sarofim AF. The effects of ferrocene addition on soot particle inception and growth in premixed ethylene flames. Combust Flame 1987;70:17–31.
[31] Uner D, Demirkol MK, Dernaika B. A novel catalyst for diesel soot oxidation. Appl Catal B – Environ 2005;61:334–45.
[32] Hai W. Formation of nascent soot and other condensed-phase materials in flames. Proc Combust Inst 2011;33:41–67.
[33] Manoj B, Sreelaksmi S, Mohan AN, Kunjomana AG. Characterization of diesel soot from the combustion in engine by X-ray and spectroscopic techniques. Int J Electrochem Soc 2012;7:3215–21.
[34] Heywood JB. Internal combustion engine fundamentals. New York: McGraw-Hill; 1988.
[35] Lapuerta M, Martos FJ, Herreros JM. Effect of engine operating conditions on the size of primary particles composing diesel soot agglomerates. J Aerosol Sci 2007;38:455–66.
[36] Koylu UO, McEnally CS, Rosner DE, Pfefferle LD. Simultaneous measurements of soot volume fraction and particle size/microstructure in flames using a thermophoretic sampling technique. Combust Flame 1997;110:494–507.
[37] Koylu UO, Xing YC, Rosner DE. Fractal morphology analysis of combustion-generated aggregates using angular light scattering and electron microscope images. Langmuir 1995;11:4848–54.
[38] Meakin P. On growth and form. Boston: Martinus-Nijhoff; 1986.
[39] Lee KO, Cole R, Sekar R, Choi MY, Kang JS, Bae CS, et al. Morphological investigation of the microstructure, dimensions, and fractal geometry of diesel particulates. Proc Combust Inst 2002;29:647–53.
[40] Bellamy LJ. The infrared spectra of complex molecules. London: Chapman and Hall; 1975.
[41] Fernandes MB, Skjemstad JO, Johnson BB, Wells JD, Brooks P. Characterization of carbonaceous combustion residues. I. Morphological, elemental and spectroscopic features. Chemosphere 2003;51:785–95.
[42] McBeath AV, Smernik RJ, Schneider MPW, Schmidt MWI, Plant EL. Determination of the aromaticity and the degree of aromatic condensation of a thermosequence of wood charcoal using NMR. Org Geochem 2011;42:1194–202.
[43] Smernik RJ, Oades JM. The use of spin counting for determining quantitation in solid state 13C NMR spectra of natural organic matter: 1. Model systems and the effects of paramagnetic impurities. Geoderma 2000;96:101–29.